Fish & Shellfish Immunology 39 (2014) 99–107

Contents lists available at ScienceDirect

Fish & Shellfish Immunology

journal homepage: www.elsevier.com/locate/fsi

Full length article

Identification of a novel molluscan short-type peptidoglycan recognition protein in disk abalone (*Haliotis discus discus*) involved in host antibacterial defense

H.K.A. Premachandra [1], Don Anushka Sandaruwan Elvitigala [1], Ilson Whang*, Jehee Lee*

Department of Marine Life Sciences, School of Marine Biomedical Sciences, Jeju National University, Jeju Special Self-Governing Province 690-756, Republic of Korea

ARTICLE INFO

Article history:
Received 4 February 2014
Received in revised form
2 April 2014
Accepted 23 April 2014
Available online 5 May 2014

Keywords:
PGRP
Disk abalone
Genomic arrangement
Amidase and antibacterial activity
Transcriptional analysis

ABSTRACT

Peptidoglycan recognition proteins (PGRPs) are a widely studied group of pattern recognition receptors found in invertebrate as well as vertebrate lineages, and are involved in bacterial pathogen sensing. However, in addition to this principal role, they can also function in multiple host defense processes, including cell phagocytosis and hydrolysis of peptidoglycans (PGNs). In this study, a novel invertebrate short-type PGRP was identified in disk abalone (*Haliotis discus discus*) designated as AbPGRP. The complete coding sequence of *AbPGRP* was 534 bp, encoding a 178-amino acid protein with a predicted molecular mass of 20 kDa. The AbPGRP gene had a bipartite arrangement consisting of two exons separated by a single intron. Homology analysis revealed that AbPGRP shares conserved features, including amino acid residues critical for substrate and ion binding as well as for its amidase activity, with homologs of other species. Phylogenetic analysis of AbPGRP revealed that it likely evolved from a common ancestor of invertebrates, having significant homology with other molluscan PGRPs. Recombinant AbPGRP exhibited detectable, dose-dependent PGN-hydrolyzing activity with the presence of Zn^{2+}, and strong antibacterial activity against *Vibrio tapetis*, consistent with the functional properties previously reported for PGRPs in other mollusks. Moreover, *AbPGRP* transcription was induced upon treatment of healthy abalones with bacterial peptidoglycan and lipopolysaccharide, although the expression profiles differed with treatment, suggesting a capacity for discriminating between bacterial pathogens through molecular pattern recognition. Collectively, the findings of this study indicate that AbPGRP is a true homolog of invertebrate PGRPs and likely plays an indispensable role in host immunity.

1. Introduction

Peptidoglycans (PGNs) are polymers of alternating sugar molecules cross-linked by small peptides, which are abundant and essential components of the cell wall surrounding the plasma membrane in most bacterial species, most prominently in Gram-positive bacteria and to a lesser extent in Gram-negative bacteria [1]. However, bacterial PGNs can also function as evolutionarily conserved pathogen-associated molecular patterns (PAMPs), which are targeted by pattern recognition receptors (PRRs) of the eukaryotic innate immune system [2,3]. This system in higher eukaryotes, including mammals, has different types of PRRs such as CD14, Toll-like receptor 2, peptidoglycan recognition proteins (PGRPs) and some Nod-like receptors [4]. Among these, PGRPs play a significant role in triggering the immune signaling pathways, which in turn activate antimicrobial peptides, but also in cell phagocytosis and PGN hydrolysis, especially in insects [5–7]. Upon the binding of bacterial PGN, PGRPs can either inhibit or activate the downstream immune signaling pathways such as Toll and IMD pathways [8–10] or JNK pathway [11,12]. Apart from pathogen sensing, some of the PGRPs have demonstrated a prominent amidase activity by cleaving the lactylamide bond between muramic acid and peptide strand in bacterial PGN [12–14] and potent bactericidal activity against pathogenic bacteria [15] convincing their indispensable role in innate immunity. For instance, Antibacterial and amidase activities, demonstrated against PGNs by

* Corresponding authors. Marine Molecular Genetics Lab, Department of Marine Life Sciences, College of Ocean Science, Jeju National University, 66 Jejudaehakno, Ara-Dong, Jeju 690-756, Republic of Korea. Tel.: +82 64 754 3472; fax: +82 64 756 3493.
E-mail addresses: ilsonwhang@hanmail.net (I. Whang), jehee@jejunu.ac.kr, jeheedaum@hanmail.net (J. Lee).
[1] These authors contributed equally to this work.

http://dx.doi.org/10.1016/j.fsi.2014.04.018
1050-4648/

mammalian (especially human) PGRPs have already been reported [16–18]. Intriguingly, several PGRP homologs identified from insects and echinodermates were found to participate in bacteria agglutination reactions as opsonins [19,20], whereas some of the amidase-active mammalian counterparts were shown to modulate the inflammatory reactions [21].

PGRPs were initially identified in insects [22,23], and subsequently in mammals [22,24] and other vertebrates, as well as in some other invertebrate species including mollusks and echinoderms [25] (although not found in lower metazoans such as nematodes), reflecting a near-universal distribution of PGRPs in the animal kingdom. No comparable PRRs have been identified in plants [25].

Insects possess 19 different short and long-type isoforms of PGRP that are generated by alternative splicing [25]. In contrast, only four different PGRP families exist in mammals, designated as PGLYRP-1, PGLYRP-2, PGLYRP-3, and PGLYRP-4 which include short, long, and intermediate-type isoforms [24]. Most PGRPs have a carboxy-terminal amidase type 2 domain (~165 amino acids), also known as a PGRP domain, which is approximately 42% identical and 55% similar among all the animals [25]. PGRPs are predominantly secreted from cells, which is facilitated by a signal peptide, or else localized inside the cell, with the exception of some homologs such as *Drosophila* PGRP-LC [25]. All vertebrate and invertebrate amidase-active PGRPs have a conserved Zn^{2+} binding site in the peptidoglycan-binding groove, similar to that of bacteriophage type 2 amidases, containing two His, one Tyr, and one Cys residue [15,18,26]. However, in non-amidase PGRPs the Cys has been replaced by a Ser residue, which can potentially be used as a marker to predict amidase activity in PGRPs [25].

Invertebrates lack an adaptive immune system and are thus totally dependent on innate immunity for defense against pathogens. Investigating invertebrate innate immune mechanisms, such as those involving PGRPs, can provide important insight into host-pathogen interactions at the molecular level. However, mollusks are underrepresented in terms of the documented information on invertebrate PGRPs compared to that of vertebrates; especially mammals, with only a few identified in *Argopecten irradians* [27], *Solen grandis* [28], *Chlamys farreri* [29,30], *Crassostrea gigas* [31], and *Biomphalaria glabrata* [32]. The studies on short type PGRP (stPGRP) counterparts of mollusks including *A. irradians*, *C. farreri*, *S. grandis* and have demonstrated their inductive expressional responses upon PGN stimulation, further providing evidences to the potent antibacterial and amidase activities specially from *C. farreri* counterpart. In addition, one of the two stPGRP counterparts identified from *S. grandis* was detected to up-regulate even under the stress of the bacterial endotoxins like LPS [28]. However, comparative studies on molluscan PGRPs containing information on their genomic genes are found to be relatively scarce.

Abalones are marine gastropod mollusks cultivated as aquacrops, and they currently account for a considerable proportion of the yield of the commercial aquaculture industry worldwide. However, marine snails, including abalones, are sensitive to variations in environmental conditions, which can have negative effects on their survival and growth. In particular, pathogenic infections and toxicants (including carcinogens) are known to impact marine organisms, making aqua-crops such as abalones as bio indicators of aquatic ecosystems by their health and viability [33]. Numerous types of bacterial [34] and viral [35] infections have been recorded in abalone crops. Under these conditions, innate immune mechanisms enable abalones to endure pathogenic threats, at least to a certain threshold.

The present study describes the identification and molecular characterization of a short-type PGRP ortholog from disk abalone (*Haliotis discus discus*) at the sequence level, including its genomic arrangement. *AbPGRP* expression was examined in various tissues important to the physiology of the organism, as well as in response to pathogenic stress. The results demonstrate a strong correlation between the functional properties of PGRP and host immune defense.

2. Materials and methods

2.1. Identification of the complete cDNA and putative genomic DNA (gDNA) sequences

Based on sequencing data (Roche 454 genome sequencer FLX systems; DNA Link, Korea), a sequence database was established using a cDNA library generated from mRNA isolated from whole tissues of disk abalone [36]. Analysis of this database using the Basic Local Alignment Search Tool (BLAST) algorithm (http://www.ncbi.nlm.nih.gov/BLAST) identified the complete cDNA sequence of a short-type PGRP homolog, which was designated as AbPGRP.

The gene was identified at genomic level through a PCR screen of a custom-made disk abalone random shear bacterial artificial chromosome (BAC) DNA library (Lucigen, Middleton, USA), according to a previously described pooling and super pooling strategy [37]. Briefly, a target partial sequence (~200 bp) of disk abalone gDNA, determined based on the previously identified full-length cDNA sequence of *AbPGRP*, was amplified in iterative PCR reactions using different pools of disk abalone BAC DNA and the primer pair AbPGRP-qF and AbPGRP-qR (Table 1). The reaction volume of 20 μL contained 0.5 U of Ex Taq polymerase (TaKaRa Bio Inc., Japan), 2 μL of 10× Ex Taq buffer, 1.6 μL of 2.5 mM dNTPs, 75 ng of template, and 10 pmol of each primer. The thermal cycling reaction was 3 min at 94 °C, followed by 35 cycles of 94 °C for 30 s, 58 °C for 30 s, and 72 °C for 30 s, performed in a TaKaRa thermal cycler. The amplification of the target sequence was confirmed by agarose gel electrophoresis. Clones were confirmed as positive by sequencing.

2.2. In silico sequence profiling and phylogenetic analysis

The amino acid sequence encoded by the complete coding region of *AbPGRP* was determined using DNAsist 2.2 software, and domain architecture with characteristic signatures were analyzed using SMART online server (http://smart.embl-heidelberg.de/). The protein sequence was compared with orthologous sequences by

Table 1
Oligomers used in this study.

Name	Purpose	Sequence (5′ → 3′)
AbPGRP-qF	BAC library screening and qPCR of *AbPGRP*	AGAGGAGGGCATTTCAGGaGTGTTC
AbPGRP-qR	BAC library screening and qPCR of *AbPGRP*	GCCGAGGCTCCATGGTGAATG
AbPGRP-cF	ORF amplification (*Eco*RI)	GAGAGAgaattcATGTCACGGGACGACCTTCTGTTT
AbPGRP-cR	ORF amplification (*Hin*dIII)	GAGAGAaagcttCTATGCTGCAGGTTTTTCGGGAGG
Ab-RpF	qRT-PCR for ribosomal protein L5 gene	TCACCAACAAGGACATCATTTGTC
Ab-RpR	qRT-PCR for ribosomal protein L5 gene	CAGGAGGAGTCCAGTGCAGTATG

pairwise and multiple sequence alignment using EMBOSS needle (http://www.Ebi.ac.uk/Tools/emboss/align) and ClustalW2 (http://www.Ebi.ac.uk/Tools/clustalw2) programs, respectively. Some of the physicochemical parameters of AbPGRP were computed using the ExPASy prot-param tool (http://web.expasy.org/protparam), and the exon-intron architecture of the gene was predicted based on the canonical AG/GT rule. Furthermore, the phylogenetic position of AbPGRP was determined by reconstructing a phylogenetic tree using the Molecular Evolutionary Genetics Analysis (MEGA) software (version 5) [38] based on the neighbor-joining method and supported by 1000 bootstrap replications.

2.3. Preparation of recombinant AbPGRP plasmid constructs

To generate a construct containing AbPGRP fused to maltose binding protein (MBP) for recombinant protein expression, the coding sequence of *AbPGRP* was PCR-amplified using the primers AbPGRP-cF and AbPGRP-cR (Table 1) containing restriction enzyme sites for *Eco*RI and *Hin*dIII, respectively (Table 1), and cloned into the pMAL-c2X vector (New England Biolabs, Ipswich, USA). The reaction volume of 50 μL contained 5 U of Ex Taq polymerase, 5 μL of 10× Ex Taq buffer, 8 μL of 2.5 mM dNTPs, 80 ng of template, and 20 pmol of each primer. The reaction was carried out as follows; Initial denaturation at 94 °C for 3 min, followed by 35 cycles of 94 °C for 30 s, 58 °C for 30 s, 72 °C for 1 min, with a final extension of 72 °C for 5 min. The PCR product (~1.3 kb) was resolved on a 1% agarose gel; the band was excised and purified using the Accuprep gel purification kit (Bioneer Co., Korea). The digested pMAL-c2X vector (150 ng) and PCR product (180 ng) were ligated using Mighty Mix (7.5 μL; TaKaRa Bio Inc.) at 4 °C overnight. The ligation product was transformed into DH5α cells, and clones were sequenced. The plasmid was transformed into BL21 (DE3) competent cells for protein expression.

2.4. Expression and purification of AbPGRP recombinant fusion protein (rAbPGRP–MBP)

Expression and purification of rAbPGRP fused to MBP was performed according to the instructions for the pMAL Protein Fusion and Purification System supplied by the manufacturer (New England Biolabs). Briefly, rAbPGRP expression was induced with isopropyl-β-D-galactopyranoside (IPTG; 0.5 mM final concentration) in BL21 (DE3) cells grown in 500 mL LB medium supplemented with ampicillin (100 μg/mL) and glucose (0.2% final concentration) at 20 °C for 8 h. The cells were cooled on ice for 30 min and harvested by centrifugation at 3500 rpm at 4 °C for 30 min. Cells were resuspended in 20 mL column buffer (20 mM Tris-HCl, pH 7.4; 200 mM NaCl) and stored at −20 °C overnight. The following day, the cells were thawed in an ice water bath and lysed by cold temperature sonication. The lysate was centrifuged at 13,000 × g for 30 min at 4 °C; the supernatant (*i.e.*, crude extract) was mixed with 1 mL amylose resin and placed on ice for 2 h while mixing every 10 min to facilitate high affinity binding. The resin-extract mixture was loaded into a 1 cm × 5 cm column and washed with column buffer (12× volume). The rAbPGRP–MBP fusion protein was eluted with 10 mM maltose buffer, and concentration was determined by the Bradford method using bovine serum albumin as a standard [39]. The protein samples collected at different purification steps were analyzed by 12% SDS-PAGE with reducing conditions using standard size protein markers (Enzynomics, Seoul, Korea). The gel was stained with 0.05% Coomassie blue R-250, followed by a standard de-staining procedure.

2.5. Amidase activity assay

To analyze the amidase activity of AbPGRP through its PGN hydrolyzing ability, PGN from *Staphylococcus aureus* (Sigma, USA) was resuspended with different concentrations of rAbPGRP or MBP (control) to a final concentration of 1 mg/mL in HEPES buffer (20 mM, pH 7.2; 150 mM NaCl) with or without 10 μM Zn^{2+}. The mixture was incubated at 30 °C for 4 h and optical density (OD) was measured at 540 nm. The relative activity was calculated based on a standard curve generated using different concentrations of PGN. The assay was performed in triplicate to confirm the repeatability. Significant difference ($p < 0.05$) among experimental and control (MBP) assays were determined using a two-tailed paired *T*-test.

2.6. Antibacterial activity assay

To examine antibacterial activity of AbPGRP against *Vibrio tapetis*, a common bacterial pathogen of shellfish, 4 mL of bacterial cultures in exponential growth phase ($OD_{600} = 0.4–0.5$) grown in LB medium at 37 °C were pelleted by centrifugation, washed twice with PBS solution and resuspended in PBS. Cells were diluted 10^4 times in PBS and incubated with or without rAbPGRP (50 μg/mL and 25 μg/mL separately) or MBP (50 μg/mL) for 2 h. Each sample (100 μL) was plated onto LB-agar and incubated at 37 °C overnight. The number of colonies was counted, and the number of colony-forming units (CFU) per milliliter of plated cells was calculated as the mean of triplicate assays. Significant difference ($P< 0.05$) among each set of assays was determined using a two-tailed paired *T*-test.

2.7. Animal husbandry and tissue extraction

Healthy disk abalones (*H. discus discus*), with an average weight of 50 g and size of ~8 cm, were purchased from the Youngsoo abalone farm of Jeju Island (Korea). Upon arrival, the live abalones were acclimatized to the laboratory environment (seawater tanks with continuous filtering and aeration; salinity: 33 ± 1 psu; temperature: 20 ± 1 °C) for one week prior to the experiments and fed daily with fresh marine seaweed (*Undaria pinnatifida*). Hemolymph was collected from the pericardial cavities of three healthy, unchallenged abalones using sterilized syringes; samples were immediately centrifuged (3000 × g at 4 °C for 10 min) to harvest hemocytes. Tissue from adductor muscle, mantle, gill, hepatopancreas, digestive tract, and gonad was collected from three animals, snap-frozen in liquid nitrogen, and stored at −80 °C until use.

2.8. Immune challenge experiment

Acclimatized healthy abalones, reared as described in Section 2.5, were used for immune stimulation. Animals were challenged with lipopolysaccharide (LPS; *Escherichia coli* 0127:B8; Sigma) or PGN (*Staphylococcus aureus* 77140; Sigma) through intramuscular injection of 100 μL (500 μg/animal) of either mitogen, equal to a dose of approximately 10 mg/kg. Un-injected abalones, and abalones injected with the equivalent volume of saline, were used as negative controls. Gill tissue samples were collected from the animals at 3, 6, 12, 24, 48, and 72 h post-injection (p.i.). Total RNA extracted from the gill tissue of at least four animals from the immune-challenged groups and three animals from the control groups was used for cDNA synthesis to determine *AbPGRP* expression levels at the various time points.

2.9. Total RNA extraction and cDNA synthesis

Total RNA was extracted from tissue samples collected from healthy abalones (Section 2.7), and gill tissue of immune-challenged

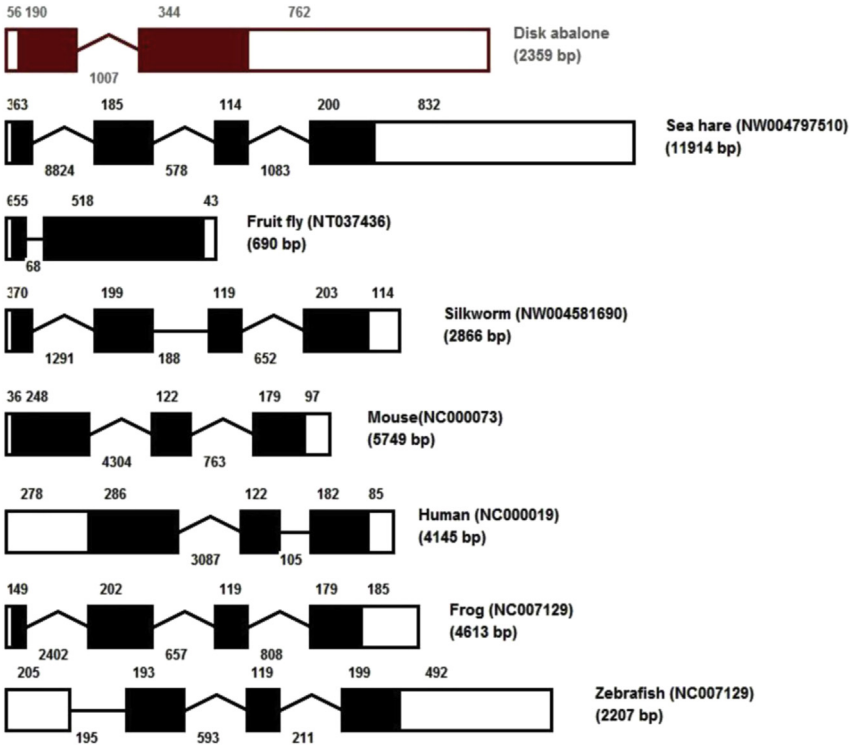

Fig. 1. Genomic organization of *AbPGRP* and PGRPs in other organisms. Exons and introns are represented by boxes and solid lines, respectively. Exon sizes are indicated above each exon, and intron sizes are indicated below each intron. Black or maroon represents coding sequences, whereas white represents UTRs. Inverted V-shaped lines (Λ) represent introns >100 bp. The NCBI GenBank accession number for the genomic sequence of each organism is shown in parentheses. (For interpretation of the references to color in this figure legend, the reader is referred to the web version of this article.)

animals, using TRI Reagent (Sigma). Concentration was measured at an optical density of 260 nm using a UV spectrophotometer (Bio-Rad, Hercules, USA). Purified RNA samples were diluted up to 1 μg/μL, and pooled to perform multi-tissue cDNA synthesis using the PrimeScript cDNA synthesis kit (TaKaRa Bio Inc.) according to the manufacturer's instructions. The cDNA was diluted 40-fold (800 μL total volume) and stored at −20 °C until use.

2.10. Analysis of AbPGRP transcript levels by quantitative real-time PCR (qPCR)

Expression of *AbPGRP* in various tissues of healthy abalones, and the temporal expression profile of *AbPGRP* in gill tissue of immune-challenged animals, was evaluated by qPCR in a Thermal Cycler Dice Real Time System (TP800; TaKaRa Bio Inc.), following the essential MIQE guidelines [40]. The 15 μL reaction volume contained 4 μL diluted cDNA from each tissue, 7.5 μL 2× TaKaRa Ex Taq SYBR Green premix, 0.6 μL each forward (AbPGRP-qF) and reverse (AbPGRP-qR) primers (Table 1), and 2.3 μL of ddH_2O. The reaction was performed as follows: 95 °C for 10 s; 35 cycles of 95 °C for 5 s, 58 °C for 10 s, and 72 °C for 20 s; and a final cycle of 95 °C for 15 s, 60 °C for 30 s, and 95 °C for 15 s. The baseline was set automatically by the Thermal Cycler Dice Real Time System software (version 2.00). *AbPGRP* expression was determined by the Livak ($2^{-\Delta\Delta CT}$) method [41]. The same qPCR program was used for the internal control, abalone ribosomal protein L5 (GenBank ID: EF103443), amplified using the appropriate primers (Table 1). Expression levels were determined relative to the control, and are presented as mean ± standard deviation (SD) of triplicate reactions. Expression level of *AbPGRP* detected for immune-challenged animals was normalized to the level in saline-injected controls to eliminate possible bias from the injection medium. The relative mRNA expression in the un-injected group was considered as the baseline. Significant differences ($p < 0.05$) between the experimental and control (un-injected) groups were determined using a two-tailed unpaired *T*-test.

3. Results and discussion

3.1. Sequence profiles and comparative analysis of AbPGRP

The complete genomic sequence of *AbPGRP* was 2359 nucleotides in length, with two exons separated by one intron (Fig. 1). The full-length cDNA sequence was 1352 bp, with 534 bp encoding a protein of 178 amino acids with a predicted molecular mass of 20 kDa and theoretical isoelectric point of 5.8, and 5′ and 3′ untranslated region (UTR) of 56 and 762 bp, respectively. Sequence data for *AbPGRP* were deposited in the NCBI GenBank database under the accession number KF554145. A comparison of the *AbPGRP* genomic sequence with vertebrate and invertebrate homologs revealed that invertebrate PGRPs had bi- and quadripartite organization, whereas in vertebrates, a tri- and quadripartite arrangement, suggesting the existence of different isoforms of PGRP (including *AbPGRP*) through alternative splicing [42]. PGRPs in invertebrate lineages displayed a more complex organization, since intron gain and loss have occurred under evolutionary pressure in different taxonomic groups, whereas vertebrates lost one intron during the evolution from lower vertebrates (*e.g.*, teleosts) to higher vertebrates (*e.g.*, mammals). Moreover, even within the same molluscan taxon, variations in gene arrangement were observed between disk abalone and sea hare, implying a diversity in PGRP function that can be explained by the existence of splice variants [42].

In silico analysis of the AbPGRP protein sequence revealed characteristic elements of the PGRP superfamily, including the

PGRP and N-acetylmuramoyl-L-alanine amidase domains (Ami_2 domain) (Fig. 2). Multiple sequence comparisons revealed that AbPGRP has some of the critical fully or partially conserved residues, such as those involved in substrate binding (His36, Thr37, Tyr70, Arg84, Ala91, His 92, Asn97, His144, Arg148, Thr150, Ala151, and Cys152); Zn^{2+} binding (His35, His144, Tyr70, and Cys152); and amidase activity (His35, Tyr70, His144, Thr150, and Cys152) (Fig. 2). AbPGRP had relatively low similarity and identity with PGRPs of other species; the highest identity was with the PGRP-2 of the mollusk *Euprymna scolopes* (44.3%), while the highest similarity was with the insect *Myrmica sulcinodis* (56.8%), demonstrating a clear homology with other invertebrate species (Table 2). These results prefigure that *AbPGRP* may encode a Zn^{2+} dependent amidase that degrades PGN to limit immune system activation upon bacterial invasion, as described previously [14,18].

3.2. Phylogeny of AbPGRP

According to the generated phylogenetic reconstruction using different vertebrate and invertebrate PGRP counterparts, two major clustered could be identified (Fig. 3). One of which represented only by invertebrate homologs, more precisely by molluscan counterparts, whereas the other contained both vertebrate and invertebrate similitudes. As expected, disk abalone PGRP (AbPGRP) was closely clustered with two molluscan homologs from squid with a strong bootstrap support (99). This observation provides substantial evidence for the homology and closer evolutionary relationship of AbPGRP with its molluscan counterparts. However, scallop PGRPS1 was diverged from the main cluster which shares the same evolutionary origin with it, displaying a phylogenetically distance relationship not only with its vertebrate counterparts but also with some molluscan similitudes including AbPGRP. It is intriguing to note that fruit fly PGRPs were clustered with its vertebrate counterparts, where some of the short-type PGRPs (PGRP-SD and PGRP-SC2) formed a separate clade with their mammalian (human and mouse PGRPs) and amphibian (frog PGLYRLP) counterparts. This clustering pattern suggests that fruit fly PGRPs shares common evolutionary origin of vertebrate PGRPs. Moreover, PGRP homologs of oyster and razor clam have clustered more closely while diverging from other molluscan counterparts to form a distinct clade in the main tree. This convinces us that these molluscan PGRPs were originated independent to the other vertebrate and invertebrate PGRPs appears in this reconstruction, in the evolutionary chronicle. Altogether, results suggest that AbPGRP is a true PGRP homolog that shares a closer evolutionary origin with invertebrate PGRPs especially that of some molluscan PGRPs, and distance phylogenetic root of vertebrate PGRPs.

3.3. Integrity and purity of rAbPGRP

Successful expression and purification of rAbPGRP-MBP was confirmed by SDS-PAGE, in which the expected protein bands corresponding to the different steps were observed (Fig. 4). The significant level of purity and integrity of the final eluted recombinant fusion protein was affirmed by the single band resolved in the gel corresponding to a ~62.5 kDa purified protein, which includes the 20 kDa rAbPGRP and ~42.5 kDa MBP.

3.4. Dose-dependent amidase activity of rAbPGRP

The amidase activity of rAbPGRP was determined based on the reduction in OD of the reaction mixture at 540 nm, resulting from the degradation of PGN. The activity was initially determined at a concentration of 1 μg/μL rAbPGRP in the presence or absence of Zn^{2+}. Hydrolytic activity against PGN in both cases (~56% and ~42% with and without Zn^{2+}, respectively) was significantly higher ($P < 0.05$) than in control reactions with MBP (Fig. 5A). Moreover, a low but detectable, dose-dependent PGN hydrolytic activity was detected in the presence of Zn^{2+} (Fig. 5B). There was negligible PGN hydrolytic activity associated with MBP. As

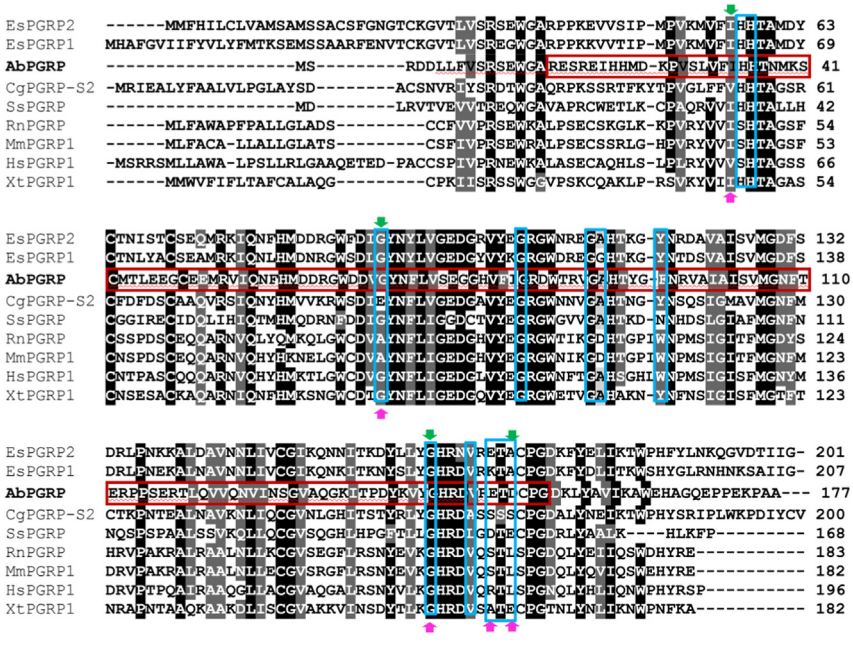

Fig. 2. Protein sequence alignment of AbPGRP with vertebrate and invertebrate PGRPs. Alignments were obtained using the Clustal-W tool. The PGRP domain is underlined with a red wavy line, and the Ami_2 domain is indicated by a maroon box. Fully or partially conserved residues are shaded in black and gray, respectively. Also shown are residues involved in substrate binding (blue box), Zn^{2+} binding (green arrows), and amidase activity (purple arrows). Es, *E. scolopes*; Cg, *C. gigas*; Ss, *Salmo salar*; Rn, *Rattus norvegicus*; Mm, *Mus musculus*; Hs, *Homo sapiens*; Xt, *Xenopus tropicalis*. (For interpretation of the references to color in this figure legend, the reader is referred to the web version of this article.)

Table 2
Percent similarity and identity of AbPGRP with its homologs.

Accession no.	Protein	Organism	Common name	Identity	Similarity	Length (amino acids)
AAY27974	PGRP2 Precursor	*Euprymna scolopes*	Hawaiian bobtail squid	44.30%	55.70%	201
AAY27973	PGRP1	*Euprymna scolopes*	Hawaiian bobtail squid	42.50%	55.60%	207
ACT66868	PGRP Precursor	*Myrmica sulcinodis*	Ant	38.40%	56.80%	178
AAH91103	PGRP1 precursor	*Xenopus tropicalis*	African clawed Frog	38.20%	50.80%	182
ACT66863	PGRP Precursor	*Myrmica sulcinodis*	Ant	38.00%	55.10%	181
BAG31898	PGRP S2	*Crassostrea gigas*	Pacific oyster	37.60%	49.50%	200
ACI69523	PGRP	*Salmo salar*	Atlantic salmon	37.10%	53.40%	168
AAH05582	PGRP	*Mus musculus*	Mouse	37.00%	54.20%	182
AAF73252	PGRP	*Rattus norvegicus*	Rat	35.80%	53.40%	183
AEH26026	PGRP	*Physella acuta*	Tadpole Snail	34.70%	47.70%	183
AAI01848	PGRP1	*Homo sapiens*	Human	34.50%	51.20%	196
ACV67267	PGRP SC2 Precursor	*Brachionus manjavacas*	Rotifer	33.80%	46.00%	203
AAY27975	PGRP3 Precursor	*Euprymna scolopes*	Hawaiian bobtail squid	33.30%	48.60%	243
BAF74637	PGRP D	*Samia cynthia ricini*	Eri silkmoth	32.80%	46.20%	237
BAG31899	PGRP S3	*Crassostrea gigas*	Pacific oyster	32.20%	42.10%	237
AFH35135	Short PGRP	*Branchiostoma japonicum*	Japanese lancelet	28.60%	40.90%	250
AAY53765	PGRP S1 Precursor	*Chlamys farreri*	Akazara scallop	28.00%	43.70%	252
AAY27976	PGRP4	*Euprymna scolopes*	Hawaiian bobtail squid	27.60%	40.10%	270
NJ642118	PGRP S1	*Solen grandis*	Razer clam	24.90%	35.40%	270
BAG31896	PGRP S1S	*Crassostrea gigas*	Pacific oyster	23.60%	31.20%	308
ACZ94668	PGRP LC isoform E	*Drosophila melanogaster*	Fruit fly	21.80%	30.70%	329
BAG31897	PGRP S1L	*Crassostrea gigas*	Pacific oyster	21.50%	28.00%	348

mentioned earlier, some PGRP superfamily members exhibit N-acetylmuramoyl-L-alanine amidase activity, which degrades PGN through cleavage of the amide bond linking the peptide to the muramic acid residues of the glycan strands [15,18,43]. Consequently, excessive activation of host immunity against invading bacteria can be aborted [12,44]. Similarly, our results on PGN hydrolysis activity of rAbPGRP along with the outcomes of sequence characterization, especially the presence of critical conserved residues suggests its putative amidase activity which may in turn important in regulation of host immune responses upon bacterial infection. Interestingly, significant Zn^{2+}-dependent amidase activity was also reported for a short-type PGRP in the mollusk *C. farreri* [30], where OD_{540} of the reaction mixture containing PGN and PGRP decreased dramatically over time when Zn^{2+} was present consisting with our observation on PGN hydrolyzing activity.

3.5. Antibacterial activity of rAbPGRP

Potential bactericidal activity of AbPGRP was investigated by determining the CFU in *V. tapetis* culture at its exponential growth phase, after the treatment of rAbPGRP. As encountered by colony counting, *V. tapetis* cultures treated with two different concentrations of the rAbPGRP-MBP fusion protein showed significantly low ($P < 0.05$) colony formation (~200 CFU/mL and ~275 CFU/mL in 50 μg/mL and 25 μg/mL treated cultures, respectively) compared to the untreated as well as MBP-treated cultures (~2000 CFU/mL) (Fig. 6), convincing the prominent *in-vitro* bactericidal activity of rAbPGRP against *V. tapetis*. However, the degree of colony formation between two rAbPGRP treated cultures was found to be almost same (no significant deference ($P < 0.05$)), independent to the treatment dose. The comparable levels of CFU for MBP-treated and untreated samples indicated that MBP did not contribute to the antibacterial activity of the rAbPGRP-MBP fusion protein.

Some human PGRPs (PGRP-1, -3, and -4) have been shown to destroy bacteria through an interaction with the cell wall, rather

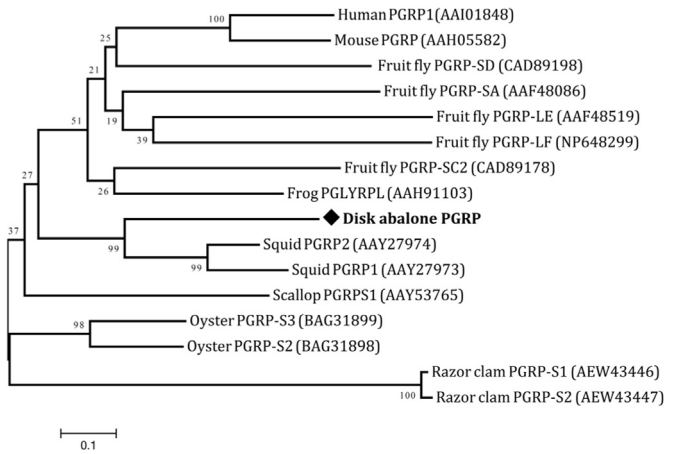

Fig. 3. Phylogenetic reconstruction of AbPGRP and vertebrate and invertebrate PGRPs based on protein sequence alignments. Distances were estimated by the neighbor-joining method using MEGA version 4.0. Bootstrap values are indicated at each node of the tree, and NCBI GenBank accession numbers are shown on each branch.

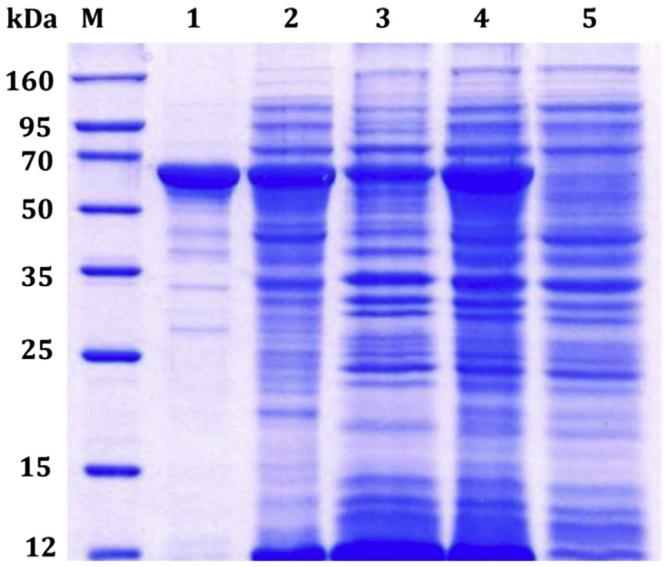

Fig. 4. SDS-PAGE analysis of each step of expression and purification of rAbPGRP-MBP fusion protein. M, protein marker; lane 1, purified rAbPGRP-MBP; lane 2, crude extract of rAbPGRP-MBP (soluble fraction); lane 3, insoluble fraction of BL21 cell extract after IPTG induction; lane 4, total cellular extract from BL21 cells after IPTG induction; lane 5, total cellular extract from BL21 cells prior to IPTG induction.

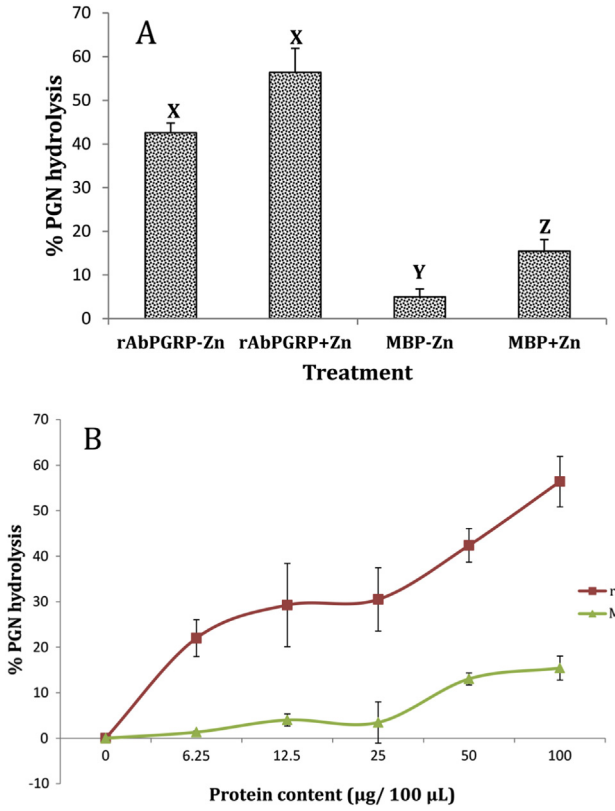

Fig. 5. Hydrolytic activity of rAbPGRP-MBP against PGN. (A) Percent PGN hydrolysis by rAbPGRP-MBP and MBP in the presence or absence of Zn^{2+}. (B) Percent PGN hydrolysis by rAbPGRP-MBP and MBP in the presence of Zn^{2+} at different protein concentrations. Error bars represent SD ($n = 3$). Significant differences ($P < 0.05$) in hydrolysis activity among control (MBP) and experimental assays in Fig. A were denoted by different letters. All the hydrolysis activities reported for the experimental assays in Fig. B were found to be significantly ($P < 0.05$) different from each corresponding control (MBP) assays.

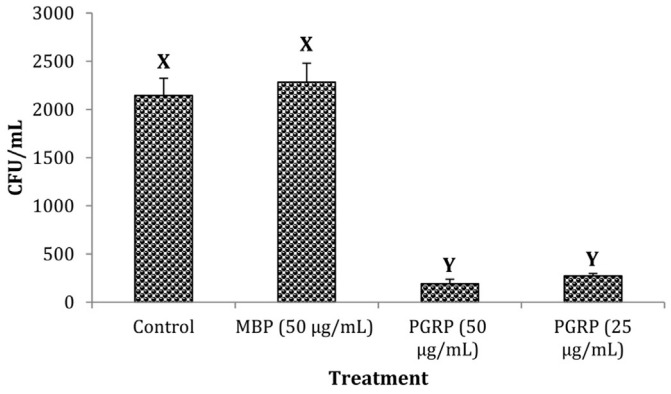

Fig. 6. Antibacterial activity of rAbPGRP-MBP and MBP as assessed by the number of colony-forming units per volume of culture (CFU/mL). Error bars represent SD ($n = 3$). Significant differences ($p < 0.05$) of CFU/mL corresponding to the each set of assays are represented by different letters.

than PGN hydrolysis or permeabilization of the cytoplasmic membrane [45]. However, this antibacterial activity was Zn^{2+}-dependent, and these PGRPs had no amidase activity [17,26]. In contrast, *Drosophila* PGRP-SC1B [15] and some PGRP variants in zebrafish [13] exhibited both amidase and antibacterial activities. Interestingly, in our case, we also could detect both amidase and antibacterial activities compatible with a previous report on PGRP counterpart from mollusk species, *C. farreri* [30], although in *H. discus discus*, these activities were Zn^{2+}-independent. Therefore, we can assume that there may be a correlation between the Zn^{2+} independent amidase and bactericidal activities of AbPGRP in a common process of host defense against invading bacteria (Fig. 5A), probably degrading the PGN on the bacterial cell wall to enhance bacteriolysis. However, further investigations are required to confirm this possibility.

3.6. Spatial expression pattern of AbPGRP

AbPGRP was ubiquitously expressed in the tissues examined; the highest transcript levels were detected in the digestive tract and hemocytes, compared to a basal expression level in muscle tissue (Fig. 7). Hemocytes are potent immune cells in mollusks, which are involved in the clearance of infections through phagocytosis or encapsulation of invading entities [46]. Moreover, hemocytes secrete humoral immunity factors including lysozymes, amino-peptidases, lectins, and antimicrobial molecules that are directly involved in the elimination of pathogens [47,48]. Therefore, the prominent expression of *AbPGRP* and antimicrobial proteins in abalone hemocytes underscore a critical role in host immunity. As reported previously, some abalone species were detected with high prevalence of intracellular Rickettsiales-like prokaryote pathogens in their digestive tracts, some of which were symptomatic [49]. On the other hand antimicrobial proteins such as lysozymes were found to express prominently in digestive cells and serve as digestive enzymes for enteric and engulfed bacteria in digestive organs, involving in host antimicrobial defense [50]. Thus, it is not unlikely to expect a prominent level expression of AbPGRP like antimicrobial proteins in disk abalone digestive tract cells to combat the potential infectious pathogenic microbes plausibly based on its bactericidal activity (Section 3.5). High levels of PGRP expression in circulating hemocytes were also reported in the mollusks *A. irradians* [27] and *C. gigas* [31], although in the former, expression was also high in gonad and kidney tissues. In another mollusk species, *S. grandis*, two PGRPs were identified; Sg-PGRP-S1 was expressed mostly in muscle and hepatopancreas, whereas SgPGRP-S2 was detected primarily in gill and mantle tissues, in contrast to what was observed in disk abalone.

3.7. Transcriptional response of AbPGRP upon pathogen-induced immune challenge

In order to evaluate the ability of AbPGRP to sense pathogens through the recognition of bacterial PAMPs, the modulation of *AbPGRP* expression in response to two different bacterial mitogens, PGN and LPS, was investigated in gill tissues. Since gills are exposed to the outer environment, they are particularly vulnerable to infection. Upon stimulation with PGN, a PAMP typically recognized by PGRPs, expression of the *AbPGRP* transcript was down-regulated during the early phase of the experiment (3 and 6 h p.i.), followed by significant up-regulation at the later phase (24 and 48 h p.i.), compared to the basal level (Fig. 8A). In contrast, injection of LPS, an endotoxin of Gram-negative bacteria stimulated *AbPGRP* expression during the early phase (6 and 12 h p.i.), whereas the transcript level returned to the baseline value by the late phase (24 and 48 h p.i.), although this response was preceded by an initial down-regulation at 3 h p.i. (Fig. 8B).

Although PGRPs are known to recognize and bind PGN and trigger downstream immune signaling cascades in host organisms, some vertebrate and invertebrate PGRPs can also effectively interact with LPS [51,52]; for instance, *Drosophila* PGRP-LC has been suggested to act exclusively as a PRR for LPS [51]. The different

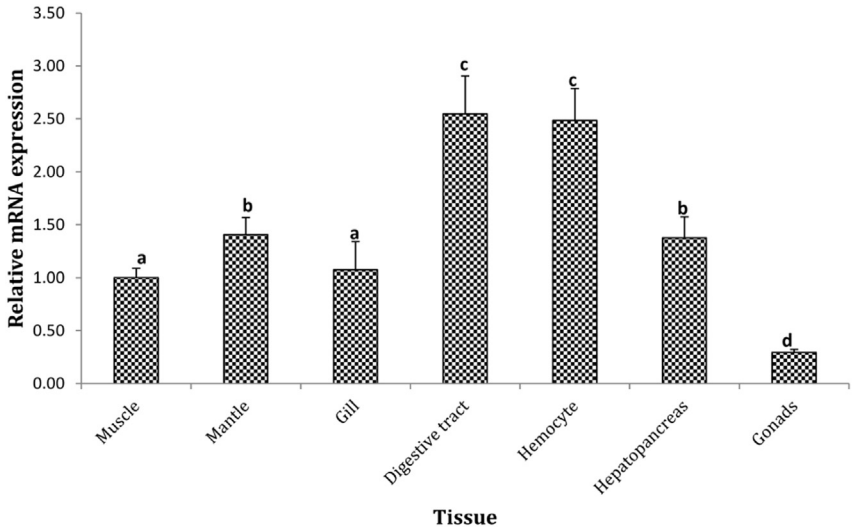

Fig. 7. Expression of *AbPGRP* transcript in various tissues of disk abalone. Fold changes of mRNA were detected by qPCR, and are presented relative to expression levels in muscle tissue. Error bars represent SD ($n = 3$). Significant differences ($P < 0.05$) in expression levels among tissues are represented by different letters.

AbPGRP transcriptional responses elicited by PGN and LPS suggest that AbPGRP preferentially recognizes LPS on bacterial cell walls, since LPS stimulated *AbPGRP* transcription at an earlier phase. Nevertheless, the induction of transcript expression by both PAMPs, combined with the PGN-hydrolyzing activity (Section 3.4), suggests that AbPGRP might act as a potent PRR in the detection of bacterial pathogens, further involving in clearance of invaded bacterial pathogens from host cells convinced by the detectable bactericidal activity (Section 3.5). However, the early down-regulation of *AbPGRP* expression in response to both PGN (3 and 6 h p.i.) and LPS (3 h p.i.) could be the result of a tolerance to endotoxins developed by immune cells in gill tissues [53,54] due to frequent contact with microbes in the outer environment.

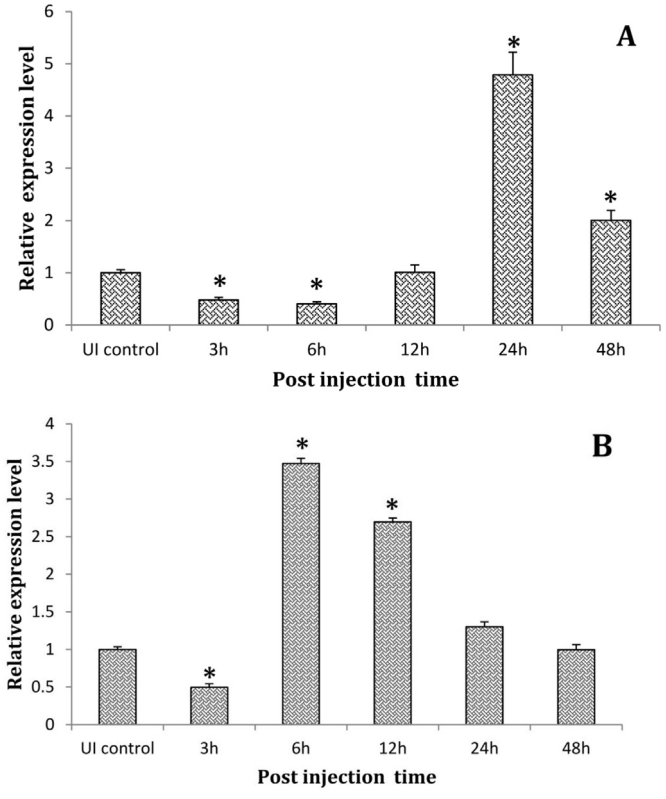

Fig. 8. Expression levels of *AbPGRP* mRNA in gill tissue upon stimulation with (A) PGN and (B) LPS. Relative mRNA expression was detected by qPCR and calculated by the $2^{-\Delta\Delta CT}$ method, using disk abalone ribosomal protein L5 as the reference gene, and normalized to the levels in saline-injected controls at each time point. The expression level in an un-injected control (UI control) was set as the baseline for comparison. Error bars represent SD ($n = 3$). *$P < 0.05$.

The transcriptional induction profile of *AbPGRP* observed in the present experiments was not consistent with what has previously been reported for other molluscan PGRPs. For instance, in *S. grandis*, SgPGRP-S1 transcription was up-regulated in hemocytes upon treatment with PGN but not with LPS [28]. In contrast, the expression of SgPGRP-S2 in hemocytes fluctuated during the early and late phases of the experiment in response to PGN, whereas clear upregulation in the early phase, followed by down-regulation in the late phase, was observed following exposure to LPS [28], being consistent with the time course of induction of *AbPGRP* by LPS. However, *PGRP* expression in *A. irradians* was unaffected by LPS treatment, while transcript levels of short-type PGRPs (PGRP-S1) in *C. farreri* [30] and *A. irradians* [27] were persistently elevated in hemocytes throughout the experiment in response to PGN. Expression of the *C. farreri* PGRP was significantly up-regulated upon LPS stimulation in the early phase of the experiment, consistent with what was observed for *AbPGRP* (Fig. 8B).

4. Conclusion

A novel invertebrate short-type PGRP was identified in the disk abalone, *H. discus discus*. The protein sequence of AbPGRP exhibited the typical domain architecture of the PGRP superfamily, with substantial similarity and identity to homologs in other mollusks and invertebrates. AbPGRP demonstrated PGN-hydrolyzing amidase activity and antibacterial activity against *V. tapetis*, consistent with the functions reported for molluscan PGRPs. The induction of *AbPGRP* transcription upon PGN and LPS treatment implies a capacity for recognizing bacterial PAMPs to generate an immune response. Taken together, the findings of this study demonstrate that AbPGRP is a *bona fide* member of the PGRP superfamily that likely plays an important role in host immune defense.

Acknowledgments

This research was supported by Golden Seed Project, Ministry of Agriculture, Food and Rural Affairs (MAFRA), Ministry of Oceans and Fisheries (MOF),Rural Development Administration (RDA) and Korea Forest Service (KFS).

References

[1] Dziarski R. Peptidoglycan recognition proteins (PGRPs). Mol Immunol 2004;40:877–86.
[2] Rosenthal RS, Dziarski R. Isolation of peptidoglycan and soluble peptidoglycan fragments. Methods Enzymol 1994;235:253–85.
[3] Schleifer KH, Kandler O. Peptidoglycan types of bacterial cell walls and their taxonomic implications. Bacteriol Rev 1972;36:407–77.
[4] Dziarski R. Recognition of bacterial peptidoglycan by the innate immune system. Cell Mol Life Sci 2003;60:1793–804.
[5] Lemaitre B, Nicolas E, Michaut L, Reichhart JM, Hoffmann JA. Pillars article: the dorsoventral regulatory gene cassette spätzle/Toll/cactus controls the potent antifungal response in *Drosophila* adults. Cell. 1996. 86: 973–983. J Immunol 2012;188:5210–20.
[6] Lemaitre B, Kromer-Metzger E, Michaut L, Nicolas E, Meister M, Georgel P, et al. A recessive mutation, immune deficiency (imd), defines two distinct control pathways in the *Drosophila* host defense. Proc Natl Acad Sci U S A 1995;92:9465–9.
[7] Werner T, Liu G, Kang D, Ekengren S, Steiner H, Hultmark D. A family of peptidoglycan recognition proteins in the fruit fly *Drosophila melanogaster*. Proc Natl Acad Sci U S A 2000;97:13772–7.
[8] Choe KM, Werner T, Stoven S, Hultmark D, Anderson KV. Requirement for a peptidoglycan recognition protein (PGRP) in relish activation and antibacterial immune responses in *Drosophila*. Science 2002;296:359–62.
[9] Hoffmann JA, Reichhart JM. *Drosophila* innate immunity: an evolutionary perspective. Nat Immunol 2002;3:121–6.
[10] Michel T, Reichhart JM, Hoffmann JA, Royet J. *Drosophila* Toll is activated by Gram-positive bacteria through a circulating peptidoglycan recognition protein. Nature 2001;414:756–9.
[11] Maillet F, Bischoff V, Vignal C, Hoffmann J, Royet J. The *Drosophila* peptidoglycan recognition protein PGRP-LF blocks PGRP-LC and IMD/JNK pathway activation. Cell Host Microbe 2008;3:293–303.
[12] Zaidman-Remy A, Herve M, Poidevin M, Pili-Floury S, Kim MS, Blanot D, et al. The *Drosophila* amidase PGRP-LB modulates the immune response to bacterial infection. Immunity 2006;24:463–73.
[13] Li X, Wang S, Qi J, Echtenkamp SF, Chatterjee R, Wang M, et al. Zebrafish peptidoglycan recognition proteins are bactericidal amidases essential for defense against bacterial infections. Immunity 2007;27:518–29.
[14] Mellroth P, Steiner H. PGRP-SB1: an N-acetylmuramoyl L-alanine amidase with antibacterial activity. Biochem Biophys Res Commun 2006;350:994–9.
[15] Mellroth P, Karlsson J, Steiner H. A scavenger function for a *Drosophila* peptidoglycan recognition protein. J Biol Chem 2003;278:7059–64.
[16] Zhang Y, van der Fits L, Voerman JS, Melief MJ, Laman JD, Wang M, et al. Identification of serum N-acetylmuramoyl-L-alanine amidase as liver peptidoglycan recognition protein 2. Biochim Biophys Acta 2005;1752:34–46.
[17] Wang M, Liu LH, Wang S, Li X, Lu X, Gupta D, et al. Human peptidoglycan recognition proteins require zinc to kill both gram-positive and gram-negative bacteria and are synergistic with antibacterial peptides. J Immunol 2007;178:3116–25.
[18] Gelius E, Persson C, Karlsson J, Steiner H. A mammalian peptidoglycan recognition protein with N-acetylmuramoyl-L-alanine amidase activity. Biochem Biophys Res Commun 2003;306:988–94.
[19] Coteur G, Mellroth P, De Lefortery C, Gillan D, Dubois P, Communi D, et al. Peptidoglycan recognition proteins with amidase activity in early deuterostomes (Echinodermata). Dev Comp Immunol 2007;31:790–804.
[20] Ramet M, Manfruelli P, Pearson A, Mathey-Prevot B, Ezekowitz RA. Functional genomic analysis of phagocytosis and identification of a *Drosophila* receptor for *E. coli*. Nature 2002;416:644–8.
[21] Saha S, Qi J, Wang S, Wang M, Li X, Kim YG, et al. PGLYRP-2 and Nod2 are both required for peptidoglycan-induced arthritis and local inflammation. Cell Host Microbe 2009;5:137–50.
[22] Kang D, Liu G, Lundstrom A, Gelius E, Steiner H. A peptidoglycan recognition protein in innate immunity conserved from insects to humans. Proc Natl Acad Sci U S A 1998;95:10078–82.
[23] Yoshida H, Kinoshita K, Ashida M. Purification of a peptidoglycan recognition protein from hemolymph of the silkworm, *Bombyx mori*. J Biol Chem 1996;271:13854–60.
[24] Liu C, Xu Z, Gupta D, Dziarski R. Peptidoglycan recognition proteins: a novel family of four human innate immunity pattern recognition molecules. J Biol Chem 2001;276:34686–94.
[25] Dziarski R, Gupta D. The peptidoglycan recognition proteins (PGRPs). Genome Biol 2006;7:232.
[26] Wang ZM, Li X, Cocklin RR, Wang M, Fukase K, Inamura S, et al. Human peptidoglycan recognition protein-L is an N-acetylmuramoyl-L-alanine amidase. J Biol Chem 2003;278:49044–52.
[27] Ni D, Song L, Wu L, Chang Y, Yu Y, Qiu L, et al. Molecular cloning and mRNA expression of peptidoglycan recognition protein (PGRP) gene in bay scallop (*Argopecten irradians*, Lamarck 1819). Dev Comp Immunol 2007;31:548–58.
[28] Wei X, Yang J, Yang D, Xu J, Liu X, Fang J, et al. Molecular cloning and mRNA expression of two peptidoglycan recognition protein (PGRP) genes from mollusk *Solen grandis*. Fish Shellfish Immunol 2012;32:178–85.
[29] Su J, Ni D, Song L, Zhao J, Qiu L. Molecular cloning and characterization of a short type peptidoglycan recognition protein (CfPGRP-S1) cDNA from Zhikong scallop *Chlamys farreri*. Fish Shellfish Immunol 2007;23:646–56.
[30] Yang J, Wang W, Wei X, Qiu L, Wang L, Zhang H, et al. Peptidoglycan recognition protein of *Chlamys farreri* (CfPGRP-S1) mediates immune defenses against bacterial infection. Dev Comp Immunol 2010;34:1300–7.
[31] Itoh N, Takahashi KG. A novel peptidoglycan recognition protein containing a goose-type lysozyme domain from the Pacific oyster, *Crassostrea gigas*. Mol Immunol 2009;46:1768–74.
[32] Zhang SM, Zeng Y, Loker ES. Characterization of immune genes from the schistosome host snail *Biomphalaria glabrata* that encode peptidoglycan recognition proteins and gram-negative bacteria binding protein. Immunogenetics 2007;59:883–98.
[33] van der Oost R, Beyer J, Vermeulen NP. Fish bioaccumulation and biomarkers in environmental risk assessment: a review. Environ Toxicol Pharmacol 2003;13:57–149.
[34] Liu PC, Chen YC, Huang CY, Lee KK. Virulence of *Vibrio parahaemolyticus* isolated from cultured small abalone, *Haliotis diversicolor supertexta*, with withering syndrome. Lett Appl Microbiol 2000;31:433–7.
[35] Nakatsugawa T, Nagai K, Hiya T, Nishizawa K, Muroga A. A virus isolated from juvenile Japanese black abalone *Nordotis discus* affected with amyotrophia. Dis Aquat Org; 1999:159–61.
[36] Lee Y, De Zoysa M, Whang I, Lee S, Kim Y, Oh C, et al. Molluscan death effector domain (DED)-containing caspase-8 gene from disk abalone (*Haliotis discus discus*): molecular characterization and expression analysis. Fish Shellfish Immunol 2011;30:480–7.
[37] Quiniou SM, Katagiri T, Miller NW, Wilson M, Wolters WR, Waldbieser GC. Construction and characterization of a BAC library from a gynogenetic channel catfish *Ictalurus punctatus*. Genet Sel Evol 2003;35:673–83.
[38] Tamura K, Peterson D, Peterson N, Stecher G, Nei M, Kumar S. MEGA5: molecular evolutionary genetics analysis using maximum likelihood, evolutionary distance, and maximum parsimony methods. Mol Biol Evol 2011;28:2731–9.
[39] Bradford MM. A rapid and sensitive method for the quantitation of microgram quantities of protein utilizing the principle of protein-dye binding. Anal Biochem 1976;72:248–54.
[40] Bustin SA, Benes V, Garson JA, Hellemans J, Huggett J, Kubista M, et al. The MIQE guidelines: minimum information for publication of quantitative real-time PCR experiments. Clin Chem 2009;55:611–22.
[41] Livak KJ, Schmittgen TD. Analysis of relative gene expression data using real-time quantitative PCR and the 2(-Delta Delta C(T)) method. Methods 2001;25:402–8.
[42] Keren H, Lev-Maor G, Ast G. Alternative splicing and evolution: diversification, exon definition and function. Nat Rev Genet 2010;11:345–55.
[43] Kim MS, Byun M, Oh BH. Crystal structure of peptidoglycan recognition protein LB from *Drosophila melanogaster*. Nat Immunol 2003;4:787–93.
[44] Bischoff V, Vignal C, Duvic B, Boneca IG, Hoffmann JA, Royet J. Downregulation of the *Drosophila* immune response by peptidoglycan-recognition proteins SC1 and SC2. PLoS Pathog 2006;2:e14.
[45] Lu X, Wang M, Qi J, Wang H, Li X, Gupta D, et al. Peptidoglycan recognition proteins are a new class of human bactericidal proteins. J Biol Chem 2006;281:5895–907.
[46] Matozzo V, Rova G, Marin MG. Haemocytes of the cockle *Cerastoderma glaucum*: morphological characterisation and involvement in immune responses. Fish Shellfish Immunol 2007;23:732–46.
[47] Aton E, Renault T, Gagnaire B, Thomas-Guyon H, Cognard C, Imbert N. A flow cytometric approach to study intracellular-free Ca^{2+} in *Crassostrea gigas* haemocytes. Fish Shellfish Immunol 2006;20:493–502.
[48] Wootton EC, Dyrynda EA, Ratcliffe NA. Bivalve immunity: comparisons between the marine mussel (*Mytilus edulis*), the edible cockle (*Cerastoderma edule*) and the razor-shell (*Ensis siliqua*). Fish Shellfish Immunol 2003;15:195–210.
[49] Caceres-Martinez J, Tinoco-Orta GD. Symbionts of cultured red abalone, *Haliotis rufescens* from Baja California, Mexico. J Shellfish Res 2001;20:875–81.
[50] Takahashi KG, Itoh N. Lysozymes in molluscs. In: Bondad-Reantaso MG, Jones JB, Corsin F, Aoki T, editors. Diseases in Asian aquaculture VII. Malaysia; 2011. pp. 93–102.
[51] Werner T, Borge-Renberg K, Mellroth P, Steiner H, Hultmark D. Functional diversity of the *Drosophila* PGRP-LC gene cluster in the response to lipopolysaccharide and peptidoglycan. J Biol Chem 2003;278:26319–22.
[52] Tydell CC, Yuan J, Tran P, Selsted ME. Bovine peptidoglycan recognition protein-S: antimicrobial activity, localization, secretion, and binding properties. J Immunol 2006;176:1154–62.
[53] Biswas SK, Lopez-Collazo E. Endotoxin tolerance: new mechanisms, molecules and clinical significance. Trends Immunol 2009;30:475–87.
[54] West MA, Heagy W. Endotoxin tolerance: a review. Crit Care Med 2002;30:S64–73.